PHILOSOPHICAL MAGAZINE LETTERS, 1999, VOL. 79, NO. 4, 195–200

A note on the amplitude–frequency relation of electromagnetic radiation pulses induced by material failure

A. RABINOVITCH

The Deichmann Rock Mechanics Laboratory of the Negev,
Physics Department, Ben Gurion University of the Negev, Beer Sheva, Israel

V. FRID and D. BAHAT

The Deichmann Rock Mechanics Laboratory of the Negev,
Department of Geological and Environmental Sciences,
Ben Gurion University of the Negev, Beer Sheva, Israel

[*Received in final form 16 December 1998 and accepted 4 January 1999*]

ABSTRACT

We have carefully analysed the amplitude–frequency relation of the electromagnetic radiation pulses emitted during the fracture of chalk, granite and glass ceramic under compression. The results show the amplitudes to be inversely proportional to the frequencies in all cases.

§ 1. INTRODUCTION

Electromagnetic radiation (EMR) from materials fractured under compression has been known since 1933 (Urosovskaja 1969). However, efforts to understand its physical origin have been unconvincing. It was considered (for example Nabarro (1967) and Finkel *et al.* (1975)) that EMR was induced by electric charges on opposite sides of elongated microdefects, resulting from the rupture of interatomic (interionic) bonds (Khatiashvili 1984). Another model for EMR was that it was caused by breakdown when charge accumulation reached a limiting value (Finkel *et al.* 1975, Gol'd *et al.* 1975, Cress *et al.* 1987). Yet another type of explanation was obtained from experiments where it was claimed that EMR was associated with the movements of charged crack sides (Miroshnichenko and Kuksenko 1980, Gershenzon *et al.* 1985). All these models provided 'qualitative' explanations but an exact quantitative theory of the properties of the detected EMR (King 1983) is still lacking.

EMR appears as individual pulses or as pulse clusters (Rabinovitch *et al.* 1995, 1996). A careful EMR pulse parametrization enabled us to associate some EMR parameters with crack dimensions (Rabinovitch *et al.* 1998).

Here we consider the hitherto untreated amplitude–frequency relations of EMR pulses from several different materials: chalk (Ramat Hovav, about 20 km from Beer Sheva, Israel), Eilat granite (Eilat, southern Israel) and glass ceramic.

Philosophical Magazine Letters ISSN 0950–0839 print/ISSN 1362–3036 online
http://www.tandf.co.uk/JNLS/phl.htm
http://www.taylorandfrancis.com/JNLS/phl.htm

§ 2. Experimental details

2.1. *Experimental equipment*

Our experimental equipment was carefully described in our previous papers (Rabinovitch *et al.* 1998, Frid *et al.* 1999) and is only briefly mentioned here. We used a triaxial load frame (TerraTeck stiff press model FX-S-33090, axial pressure up to 450 MPa and confining pressure up to 70 MPa; stiffness, 5×10^9 N m^{-1}). The confining pressure is constantly controlled by a clock-type sensor and kept constant during the loading process. The axial load is measured with a sensitive load cell (LC-222M) (maximum capacity, 220 kN). The cantilever set consisting of axial and lateral detectors (strain range, about 10) enables us to measure sample strains in three orthogonal directions parallel to the three principal stresses.

EMR was measured with a magnetic one-loop antenna of diameter 3 cm (EHFP-30 near-field probe set, Electro-Metrics Penril Corporation). It is electrically 'small' and exhibits negligible response to external electric fields. This antenna was connected via a low-noise micro-signal amplifier (Mitek Corporation Ltd; frequency range, 10 kHz–500 MHz; gain, 60 ± 0.5 dB) to a Tektronix TDS 420 digital storage oscilloscope, and then, by way of a general-purpose interface bus, to an IBM personal computer (PC).

2.2. *Experimental method*

The EMR was measured inside a thick-wall steel pressure vessel to obtain a negligible artificial noise level. Towards this aim we also used special radio-frequency filters on the power supply, independent from the industrial net power supply, and special double-screened cables (Alpha Wire Corporation Ltd) to connect the antenna via the amplifier to the storage oscilloscope.

The antenna was situated 2 cm away from the centre of the loaded samples with its normal pointing perpendicular to the cylinder axis. We monitored EMR activity in the frequency band from 10 kHz up to 50 MHz with an overall sensitivity of up to 1 μV.

Two types of rock were loaded both uniaxially and triaxially, while the glass ceramic was loaded only uniaxially. Individual EMR pulses induced by compression were observed, digitized and memorized with a storage oscilloscope and an IBM PC in real time at the moment of pulse excitation.

2.3. *Material identification*

2.3.1. *Rocks*

All rock samples were cut from a block with unified co-orientation into standard cylinders of 100 mm length and 53 mm diameter. The ends of the samples were scrupulously polished to achieve homogeneity of the stress field under compression. The end cups had a diameter identical with that of the samples. To prevent the hydrostatic loading oil from penetrating into the sample pores, all samples were jacketed by plastic jackets (Alpha Fit-221-3), and the contacts of their ends with the end cups were carefully closed. Each sample was tested with an axial strain rate of 1×10^{-5} s^{-1} and laterally by different hydrostatic oil pressures.

2.3.1.1. *Chalk.* Our samples were drilled from Middle Eocene layers along Wadi Naim in the Beer Sheva syncline (Bahat 1991). The density of all investigated samples was 2.16 ± 0.01 kg m^{-3}.

The strength of chalk under compression varies considerably, from values of around 1 MPa when wet to some 50 MPa when extremely dry. Therefore, we applied a strict drying process to our samples which involved a cycle of heating to 110°C for 24 h, and then immediate removal to a desiccator to avoid any water absorption by the samples. The axial pressures varied from 30 to 60 MPa, and the confining pressure from 0 to 5 MPa.

2.3.1.2. *Granite.* For our investigation we used a large Eilat granite 'block' from the Nahal Shelomo area of southern Israel, nearly 3 km from Eilat. This granite is grey and consists of potassium-feldspars (about 40%), quartz (about 35%) albite-oligoclase (about 20%) and biotite (about 3–4%). It is medium to coarse grained (feldspars and quartz, 2–4 mm; biotite, 0.5–1 mm) and non-porphyritic (Bogosh *et al.* 1997).

The density of all investigated samples was 2.604 ± 0.005 kg m^{-3}. The axial pressures varied from 110 to 284 MPa, and the confining pressure from 0 to 14 MPa.

2.3.2. *Glass-ceramic*

We used a β-quartz solid solution glass-ceramic. The composition of this material (Vision by Corning) in weight per cent is as follows: SiO_2, 68.8; Al_2O_3, 19.2; Li_2O, 2.7; MgO, 1.8; ZnO, 1.0; TiO_2, 2.7; ZnO_2, 1.8, plus additional traces (Beall 1989). The glass-ceramic is close to single-phase crystals of β-quartz solid solution about 600 Å (60 nm) in diameter and a small amount of zirconium titanate crystals (less than 100 Å in diameter) which allow efficient light transmission (Beall 1989). The resistance to failure under uniaxial compression of samples which comply with the standard specification dimensions (106 mm length and 52 mm diameter) is very high (greater than 450 MPa) and is beyond the load capacities of our press machine. Since our purpose was to overcome the resistance to fracture and to induce controlled cracking (rather than to obtain accurate strength results), we selected a sample geometry which deviates from standard specifications. The best results were obtained on a sample with the following specifications: a length of 104 mm and having a frustum shape (the part of a conical solid left after cutting off a top portion by a plane parallel to the base) and an elliptical cross-section, such that the large and small diameters at the base end are 33 and 21 mm respectively, and the two diameters at the top end of the frustum are 33 and 10 mm respectively. The abraded flexural strength of the β-quartz solid solution glass-ceramic is 69.3 MPa (Beall *et al.* 1967). The axial pressures varied from 0 to 112 MPa (there was no confining pressure in this case).

§ 3. Experimental results

As was shown (Rabinovitch *et al.* 1998), the amplitude of an EMR pulse induced by compression fissure can be expressed by the following relationship:

$$A = \begin{cases} A_0 \sin[\omega(t-t_0)]\left[1-\exp\left(\dfrac{-(t-t_0)}{\tau}\right)\right], & t < T, \\ A_0 \sin[\omega(t-t_0)]\exp\left(\dfrac{-(t-T)}{\tau}\right)\left[1-\exp\left(\dfrac{-(T-t_0)}{\tau}\right)\right], & t \geqslant T, \end{cases} \quad (1)$$

where t is the time, t_0 is the time from the origin up to the start of the pulse and T is the time from the origin up to the EMR pulse envelope maximum. Thus,

$T' = T - t_0$ is the time interval to reach the pulse maximum, τ is the rise-and-fall time (RFT) (the rise time and the fall time turn out to be the same), A_0 is the pulse amplitude and ω is the frequency. The amplitude of the envelope of the EMR pulse is therefore determined by the following relation:

$$\bar{A} = A_0 \left[1 - \exp\left(\frac{-T'}{\tau} \right) \right]. \tag{2}$$

It was shown (Rabinovitch *et al.* 1998) that the frequency of the EMR pulses is inversely proportional to crack width. Since A_0 is proportional to the crack area, it is expected that $\bar{A} \propto 1/f$.

The voltages of the EMR pulses depend on the antenna reaction (antenna efficiency) which changes with frequency. Compensating for this factor $E = f(\bar{A})$ (E being the field amplitude reaching the antenna) by the appropriate antenna efficiency chart (EHFP-30 near field probe set, Electro-Metrics Penril Corporation), we are able to compare the heights of the various EMR signals having different frequencies.

Figure 1 shows the compensated amplitudes E of the electromagnetic field signals induced by the fracture of chalk, granite and glass-ceramic samples. Analysis of about 160 pulses shows that the amplitude–frequency ratio of each of the three materials can be fitted by a power-law-type relation. Thus, for chalk, the relation is $E \approx 6 \times 10^8 f^{-0.91 \pm 0.04}$ (squared regression coefficient $R^2 = 0.87$), for granite, $E \approx 3 \times 10^9 f^{-0.99 \pm 0.04}$ ($R^2 = 0.89$) and for the glass-ceramic, $E \approx 2 \times 10^{11} f^{-1.32 \pm 0.11}$ ($R^2 = 0.82$).

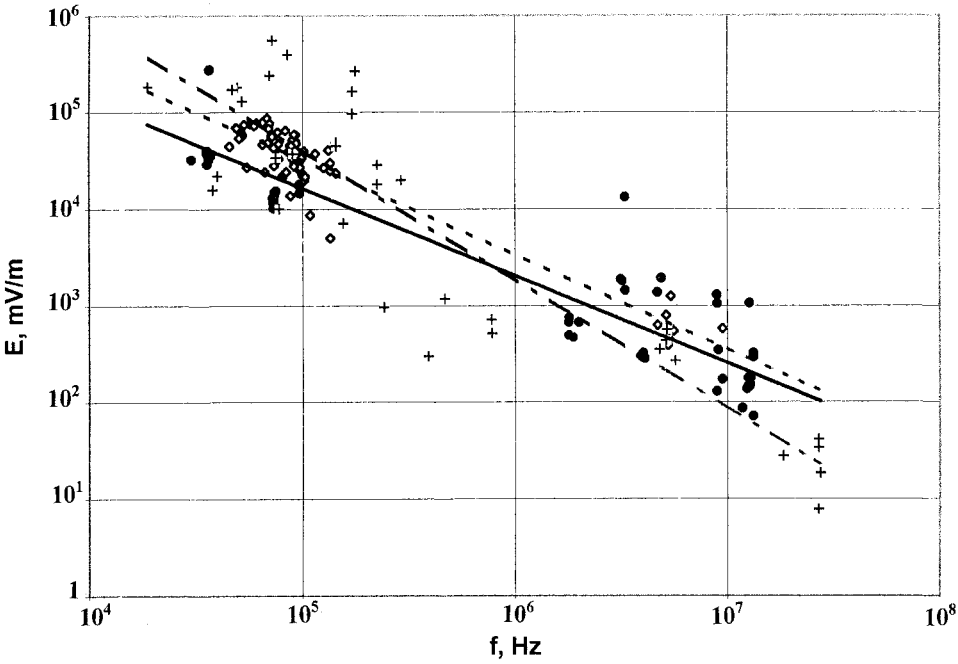

Figure 1. Amplitude–frequency relation of EMR pulses associated with chalk, granite and glass-ceramic compression: (●), chalk (◇), granite; (+), glass-ceramic; (——), chalk trend line; (– – –), granite trend line; (– - –), glass-ceramic trend line.

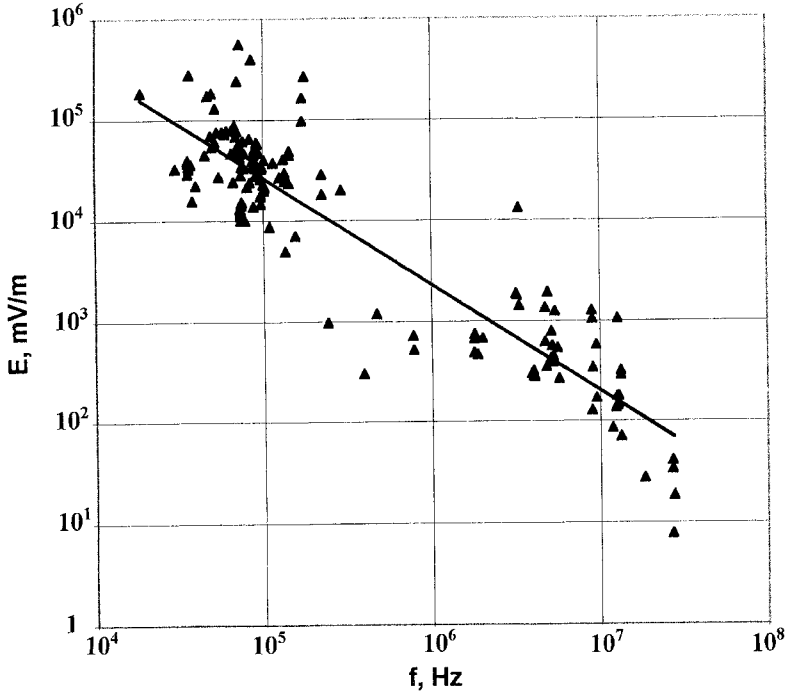

Figure 2. General amplitude–frequency relation of chalk, granite and glass-ceramic samples.

The exponents of these three relationships are very close to unity, although for the glass-ceramic the value is somewhat scattered. EMR pulses induced by chalk and granite fracture could generally be fitted by a single frequency. In contrast, some EMR pulses associated with glass-ceramic fracture were 'multifrequency'. Therefore the amplitude–frequency ratios of these pulses were corrected in the following way. The amplitude at a specific frequency peak of the fast Fourier transform was calculated from $E(f_i) = EA_i / \sum_i A_i$, where A_i is the area under the ith peak and E is the measured pulse amplitude. Such a procedure evidently adds errors; it increases the spread of the glass-ceramic results and could also be the reason for the deviant exponent. If we collect all EMR data on one figure (figure 2), a single combined relation can be obtained: $E \approx 5 \times 10^9 f^{-1.06 \pm 0.04}$ ($R^2 = 0.84$).

These results imply that the amplitude of the EMR field is inversely proportional to the signal frequency and hence to the crack width (Rabinovitch *et al.* 1998).

The final measured amplitude obviously depends also on other parameters such as the fracture length, the geometry of antenna-fracture orientation, and the attenuation along the path. These factors constitute the source of the (rather large) vertical spread in the results of figures 1 and 2.

ACKNOWLEDGEMENTS

We would like to thank the Earth Sciences Administration of the Ministry of Energy and Infrastructure and the Koret Foundation for supporting our research.

References

Bahat, D., 1991, *Tectonofractography* (Heidelberg: Springer).

Beall, G. H., 1989, *Rev. solid st. Sci.*, **3**, 333.

Beall, G. H., Karstetter, B. R., and Rittler, H. L., 1967, *J. Am. Ceram. Soc.*, **50**, 99.

Bogosh, R., Bourne, J., Shirav, M., and Harnois, L., 1997, *Mineralog. Mag.*, **61**, 111.

Cress, G. O., Brady, B. T., and Rowell, G. A., 1987, *Geophys. Res. Lett.*, **14**, 331.

Finkel, V. M., Golovin, Y. I., and Mogila, P. G., 1975, *Soviet Phys. solid State*, **17**, 492.

Frid, V., Rabinovitch, A., and Bahat, D., 1999, *Phil. Mag. Lett.*, **79**, 79.

Gershenzon, N., Zilpimiani, D., and Maguladze, P., 1985, *Dokl. Akad. Nauk. SSSR*, **288**, 75.

Gol'd, R. M., Markov, G., and Mogila, P. G., 1975, *Izv. Earth Phys.*, **7**, 109.

Khatiashvilli, N., 1984, *Izv. Earth Phys.*, **20**, 656.

King, C. Y., 1983, *Nature*, **301**, 377.

Miroshnichenko, M., and Kuksenko, V., 1980, *Soviet Phys. solid State*, **22**, 895.

Nabarro, B., 1967, *Theory of Crystal Dislocations* (Oxford University Press).

Rabinovitch, A., Bahat, D., and Frid, V., 1995, *Int. J. Fract.*, **71**, 33; 1996, *Z. Geol. Wiss.*, **24**, 361.

Rabinovitch, A., Frid, V., and Bahat, D., 1998, *Phil. Mag. Lett.*, **5**, 289.

Urusovskaja, A. A., 1969, *Soviet Phys. Usp.*, **11**, 631.